

Thermal-energy atom-scattering study of Pb submonolayers on Cu(110)

Christophe de Beauvais, Didier Rouxel, Bernard Bigeard, and Boyan Mutaftschiev

Laboratoire Maurice Letort, Centre National de la Recherche Scientifique, 54600 Villers-les-Nancy, France

(Received 4 December 1990)

Submonolayers of Pb deposited at room temperature on a Cu(110) substrate undergo, with increasing Pb coverage, a continuous transition [lattice gas $\rightarrow c(2 \times 2)$ structure], followed by a first-order transition [$c(2 \times 2) \rightarrow p(4 \times 1)$]. The further transformation of the $p(4 \times 1)$ layer into a quasicompact hexagonal layer with $p(5 \times 1)$ structure occurs by elimination of domain walls, probably with intermediate formation of a $p(9 \times 1)$ structure.

The use of thermal-energy atom scattering (TEAS) in studying the heteroepitaxy of metals on metal surfaces has been reported recently by Sanchez *et al.*¹ for the case of Pb/Cu(100). The great possibilities of this method, some of which are stressed in what follows, motivated us to consider the system Pb/Cu(110) already investigated by other techniques.

Submonolayers of Pb, deposited at room temperature on Cu(110), display by increasing surface coverage, according to the LEED and AES studies of Rhead and co-workers,^{2,3} the sequence of commensurate structures $c(2 \times 2) \rightarrow p(4 \times 1) \rightarrow p(5 \times 1)$. Further Pb condensation proceeds by formation of three-dimensional clusters on top of the first monolayer (Stranski-Krastanov growth). A more recent work on Pb films up to five monolayers (ML) thick, using the grazing-incidence x-ray technique^{4,5} and higher substrate temperatures, revealed that a quasicompact two-dimensional structure is stable up to this thickness. It melts reversibly at temperatures increasing from 490 to 590 K when the coverage decreases from 2 ML to slightly less than 1 ML. Below this coverage a phase, incommensurate in the [110] direction, is formed showing a reversed trend of melting temperatures. Formation of presumably three-dimensional crystallites (whose melting temperature is, however, still lower by 80 K than that of the bulk lead, 600.7 K) occurs only at coverages above 5 ML.

The results of the present work not only corroborated the earlier results of Rhead and collaborators,^{2,3} but also supplied information on the order of the different two-dimensional transitions and on the state and perfection of the as-formed phases. The hope to gain further insight into the complex behavior of the system at higher coverages and temperatures by TEAS seems justified.

The experimental setup enabled the scattering of the helium beam from the sample surface under continuous Pb flux of a Knudsen cell within the intensity range of 2×10^{11} to 2×10^{12} atoms $\text{cm}^{-2} \text{s}^{-1}$, thus ensuring precision of about 0.01 ML regarding the degree of coverage. The supersonic beam with a kinetic energy of 63 meV was produced by the expansion of helium from an initial pressure of 80 bars at room temperature in an IVG-Jülich-type source⁶ (energy spread of about 3%). The transfer width associated with the measurement of the scattered beam intensity I , by a Bayard-Alpert stag-

nation gauge with an aperture of 0.5° , was about 200 \AA^2 . Intensity ratios I/I_0 (I_0 being the incident flux intensity) down to 10^{-5} could be measured.

In Fig. 1(a) are plotted the specular intensity attenuations in the [110] and the [100] directions, under the in-

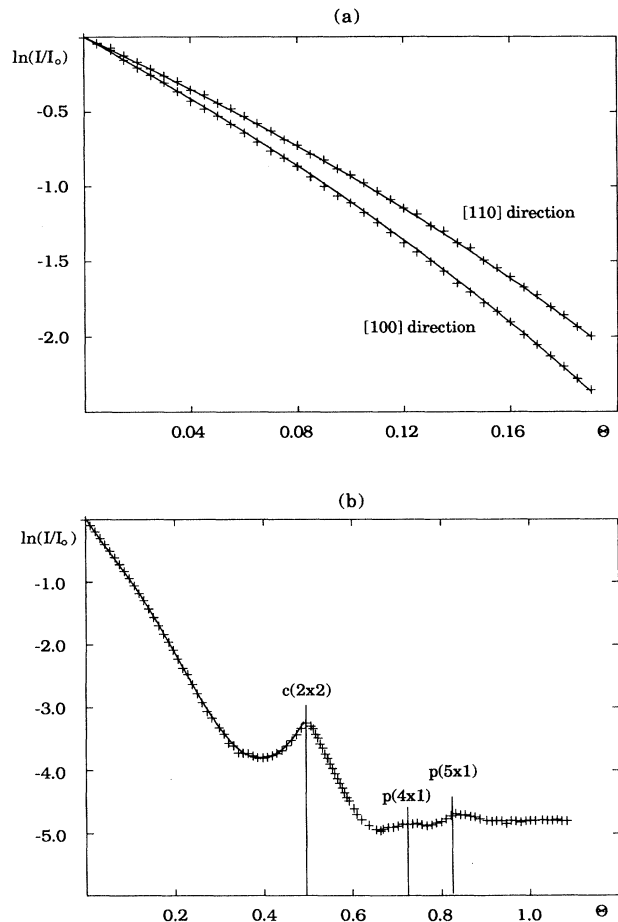


FIG. 1. (a) Attenuation of the incident beam intensity in the [110] and the [100] directions at incident angle of 52.5° , as a function of the Pb coverage. The solid lines represent the fit with Eq. (1). (b) Same as (a) at an incident angle of 45° and in the [100] direction only. The solid line gives the fit with Eq. (2) up to the formation of the $c(2 \times 2)$ structure at $\Theta = 0.5$.

cidence angle $\omega_i = 52.5^\circ$, versus lead coverage Θ , defined as the ratio between the number of Pb atoms and Cu atoms on the same surface area. Figure 1(b) represents a similar type of curve, taken in the [100] direction under an incident angle of 45° and extended to lead coverage beyond the monolayer. One can notice the presence of three maxima at coverages corresponding to the already mentioned $c(2 \times 2)$, $p(4 \times 1)$, and $p(5 \times 1)$ structures, the latter at $\Theta = 0.8$ being an almost complete Pb monolayer (cf. Fig. 2). The further condensation, presumably by formation of three-dimensional crystallites, can only slightly affect the specular beam intensity.

The experimental data of Fig. 1(a) can be perfectly fitted with the equation

$$\frac{1}{I_0} = (1 - m\Theta)^{\Sigma_{\text{Pb}}/m\Sigma_{\text{Cu}}} \quad (1)$$

proposed by Poelsema and Comsa⁷ for the case of a lattice gas of adsorbed atoms, where Σ_{Pb} and Σ_{Cu} are, respectively, the effective scattering cross sections of Pb and Cu [the latter being the area of the primitive cell of Cu(110), $\Sigma_{\text{Cu}} = 9.2 \text{ \AA}^2$], and m is the number of sublattices of equivalent adsorption sites available for adsorption ($m = 2$ in our case). From the slope at the origin of those curves one obtains for the scattering cross sections of the Pb atoms in the [110] and [100] directions the respective values of 77 and 91 \AA^2 , the difference being probably due to the anisotropy in the vibrational amplitudes along and perpendicular to the hills and valleys constituting the Cu(110) surface. The comparable large Σ_{Pb} values, 80 \AA^2 , obtained by Sanchez *et al.*¹ for Pb/Cu(100), are typical for He scattering in a number of cases.⁸⁻¹⁰

Another important feature of Fig. 1(b) is the good fit of the experimental points up to the formation of a complete $c(2 \times 2)$ overlayer, with the curve issued from the equation⁷

$$\frac{I}{I_0} = (1 - 2\Theta)^{F_{\text{Pb}}n_s} + \left(\frac{A_{\text{Pb}}}{A_0} \right)^2 (2\Theta)^{F_{\nu}n_s} + 2 \frac{A_{\text{Pb}}}{A_0} (1 - 2\Theta)^{F_{\text{Pb}}n_s/2} (2\Theta)^{F_{\nu}n_s/2} \cos\varphi, \quad (2)$$

which takes into account not only the geometrical obstruction, typical for low coverages, of part of the surface by adsorbed Pb atoms [as does Eq. (1)], but also the interference between the beams reflected from the bare and covered areas of the Cu surface. Here A_0 and A_{Pb} are the amplitudes of those beams, F_{Pb} and F_{ν} are the quantum cross sections of the Pb atoms and of the vacancies in the $c(2 \times 2)$ layer, equal to half the geometric cross sections Σ_{Pb} and Σ_{ν} ,¹¹ and $n_s = 1/\Sigma_{\text{Cu}}$ is the number of Cu atoms per unit area. φ is the phase difference,

$$\varphi = 2\pi(2h \cos\omega_i)/\lambda, \quad (3)$$

h being the effective height of the layer and λ the wavelength $\lambda = 0.57 \text{ \AA}$.

In the absence of an experimental value for h (it can be obtained from scattered intensity measurements at a variable incident angle), the fit of the experimental points of

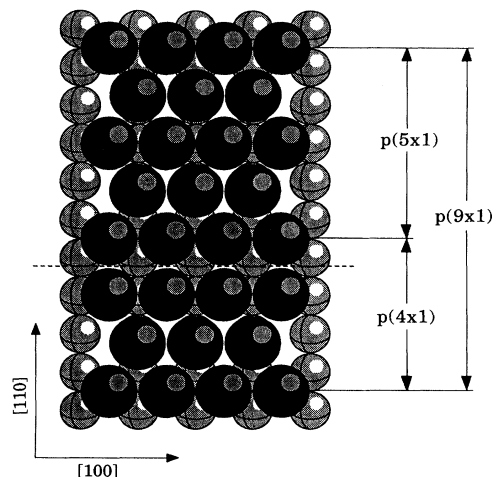


FIG. 2. Model of the $p(4 \times 1)$ and $p(5 \times 1)$ structures. The lengths indicated by the arrows are the dimensions of the unit cells in the [110] directions. One notices that the $p(9 \times 1)$ structure appears by alternation of $p(4 \times 1)$ and $p(5 \times 1)$ unit cells. The exact position of the atoms which are not situated in the potential wells of the Cu surface (at the extremities of the unit cells) could be different from that schematized on the figure (Ref. 5). Dashed line, domain wall with orientation [100].

Fig. 1(b) with Eqs. (2) and (3) was performed by leaving this parameter as the only variable. The solid line of the same figure is obtained with $h = 1 \text{ \AA}$, which is quite a reasonable value.⁷

With Eq. (2) being deduced under the assumption of a simple compression of a two-dimensional lattice gas, one may conclude that the $c(2 \times 2)$ structure (of coverage equal to one-half) is established following a continuous transition during which the adsorbed Pb atoms are under the long-range repulsion of their peers. Monte Carlo simulation of this transition, using a repulsive electrostatic potential (dipole-dipole interaction) between Pb atoms and a Lennard-Jones potential between Pb atoms and Cu atoms, indicated that $c(2 \times 2)$ is likely to be the first ordered structure obtained by compression of the lattice gas.

The decrease of the specular intensity in Fig. 1(b) for coverages between 0.5 and 0.6 can be due to either the formation of a two-dimensional lattice gas of Pb atoms on top of the $c(2 \times 2)$ layer, or the progressive disordering of this layer through the insertion of Pb atoms. Assuming the first mechanism, we were also able to fit this part of the curve with Eq. (1). The reasons why the deduced effective scattering cross section (120 \AA^2) is somewhat different from that of the first adlayer are not yet clear. The measured constant full width at half maximum (FWHM) of the scaled (20) peak profiles in this coverage range leads us to exclude the second mechanism.

Figure 3 represents the diffraction spectra in the [110] direction of Pb overlayers with coverages (a) between 0.60 and 0.70, and (b) between 0.65 and 0.80. Note that the peaks in these spectra are indexed with respect to the two-dimensional unit-cell sizes of the corresponding Pb structures.

The transition $c(2 \times 2) \rightarrow p(4 \times 1)$, demonstrated by the series of Fig. 3(a), is likely to be a first-order one. Although the $c(2 \times 2)$ structure is represented in these spectra only by the $(\bar{2}0)$ peak [which is, moreover, confused with the $(\bar{4}0)$ peak of the $p(4 \times 1)$ structure], this peak displays a rather peculiar behavior. While the ratio between the areas under the $(\bar{2}0)$ and the $(\bar{1}0)$ peaks of the $p(4 \times 1)$ structure (≈ 0.3) is roughly equal to that (≈ 0.4) under the $(\bar{3}0)$ and the $(\bar{1}0)$ peaks and is coverage independent, the ratio between the areas under the $(\bar{4}0)$ and the $(\bar{1}0)$ peaks decreases from 11 to 0.3 when the degree of coverage increases from $\Theta = 0.61$ to 0.70. One should state, therefore, that within this coverage range the $c(2 \times 2)$ and the $p(4 \times 1)$ structures are coexisting but their relative importance on the surface is changing continuously.

The $p(4 \times 1) \rightarrow p(5 \times 1)$ transition, illustrated by the spectra of Fig. 3(b), looks much more complex. The emergence of a peak at $k_{\parallel} = 0.55 \text{ \AA}^{-1}$, which coexists at $\Theta = 0.73$ with the (10) peak of the $p(4 \times 1)$ structure, suggests a first-order transition, while the continuous shift of

the former peak at higher coverages toward the position of the (10) peak of the $p(5 \times 1)$ structure could indicate the presence of an intermediate (possibly incommensurate) (Ref. 5) phase that transforms continuously to $p(5 \times 1)$.

A first-order phase transition resulting in an incommensurate phase of variable density seems highly improbable to us. Moreover, the peak at $k_{\parallel} = 0.55 \text{ \AA}^{-1}$ could be the (20) peak of a $p(9 \times 1)$ structure, obtained by the combination of one $p(4 \times 1)$ unit cell with one $p(5 \times 1)$ unit cell, as seen from the model of Fig. 2. A crude kinematic intensity calculation shows that the (10) peak of the $p(9 \times 1)$ structure should not appear. Accordingly, the physical picture of the formation of the almost compact hexagonal $p(5 \times 1)$ overlayer could be the following: first-order transformation $p(4 \times 1) \rightarrow p(9 \times 1)$; continuous annihilation of $[100]$ domain walls contained in the $p(9 \times 1)$ structure (cf. Fig. 2), leading most probably to a coarse $p(5 \times 1)$ layer.

The latter statement is supported by the results presented in Figs. 4(a) and 4(b), relative to the evolution of the peak intensities of the (quasicompact) $p(5 \times 1)$

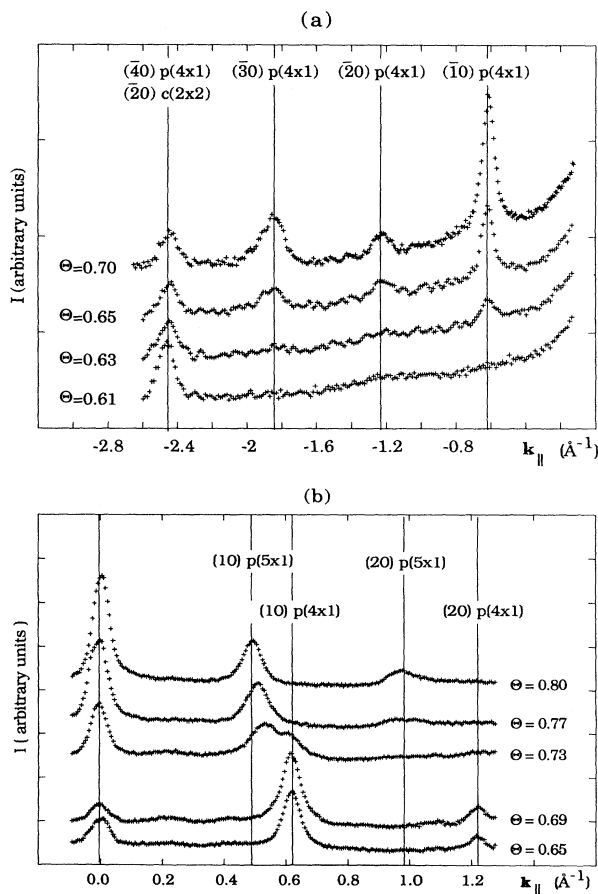


FIG. 3. (a) Diffraction spectra in the $[110]$ direction (incident angle of 65°) at different coverages corresponding to the transition $c(2 \times 2) \rightarrow p(4 \times 1)$. (b) Same as (a) at an incident angle of 59° and coverages corresponding to the $p(4 \times 1) \rightarrow p(5 \times 1)$ transition. $k_{\parallel} = k_{\parallel f} - k_{\parallel i}$, where $k_{\parallel f}$ and $k_{\parallel i}$ are the wave vectors parallel to the surface of the diffracted and incident beams, respectively.

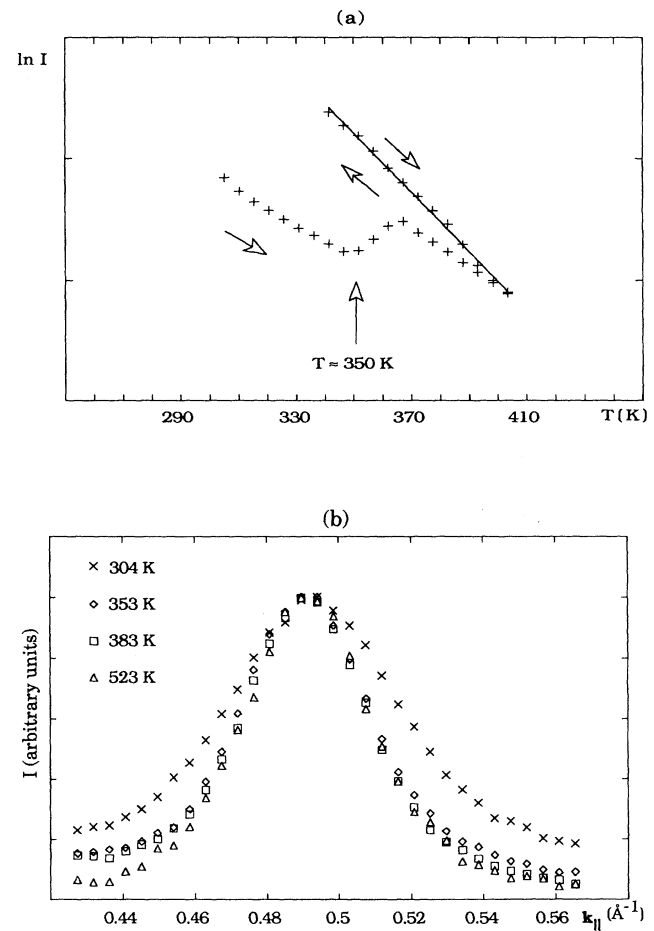


FIG. 4. (a) Incident beam intensity vs temperature at a Pb coverage slightly exceeding the monolayer. The points and arrows show the experimental path discussed in the text. (b) Scaled diffracted beam intensity of the (10) peak of the $p(5 \times 1)$ structure ($[110]$ direction, incident angle 59°) vs temperature.

structure by increasing substrate temperature. The Debye-Waller plot of Fig. 4(a), concerning an overlayer grown at room temperature and subsequently heated, shows a nearly linear part up to a temperature of 350 K followed by an intensity increase until a new straight line is reached. Further substrate temperature variations result in intensity values situated along the same straight line. In parallel, the scaled profiles of the (10) peak of the same structure [Fig. 4(b)] show a strong decrease of the FWHM in the temperature range 304–353 K.

Both the improvement of reflectivity and the sharpening of the diffraction peaks of the low-temperature-grown $p(5 \times 1)$ layer after annealing at 350 K clearly indicate the increase of the average size of its coherent domains.

When Pb is condensed at a substrate temperature of 383 K, the (10) peak of the $p(4 \times 1)$ structure shifts continuously to that of the $p(5 \times 1)$ structure. Under these conditions the hypothetical $p(9 \times 1)$ structure might not be stable.

In conclusion, the TEAS monitored deposition of Pb overlayers on the Cu(110) substrate at room temperature provides quantitative information on the very first stages of formation of the condensed $c(2 \times 2)$ phase from the lattice gas of adsorbed Pb atoms. The further increase of the Pb coverage results in the formation of a new lattice gas on top of the $c(2 \times 2)$ structure. Only when this gas is compressed to about 0.1 ML (between total coverages $\Theta = 0.5$ and 0.6) does it contribute to the first-order transformation of the $c(2 \times 2)$ layer into a $p(4 \times 1)$ layer. The transition from this structure to the quasicompact hexag-

onal $p(5 \times 1)$ structure should occur by annihilation of [100] two-dimensional domain walls. It passes, apparently, through a $p(9 \times 1)$ structure which is stable at room temperature, while at 383 K the transition $p(4 \times 1) \rightarrow p(5 \times 1)$ is continuous. So far it is difficult to say whether or not the random elimination of domain walls and the relatively small structural differences of the intermediate phases, which can be considered as mixtures of $p(4 \times 1)$ and $p(5 \times 1)$ unit cells, can explain the continuous shift of the (10) peaks. It seems, however, quite improbable that the small density modification during the $p(4 \times 1) \rightarrow p(5 \times 1)$ transition, consisting in the slip of narrow [100] bands (cf. Fig. 2) and the insertion of a new row of Pb atoms in every 15 rows of the same orientation, can be assimilated to the formation of a homogeneous incommensurate two-dimensional phase with variable density.

The authors are indebted to Y. Lejay from Commissariat à l'Énergie Atomique-Saclay and to R. David from Institut für Vakuumphysik and Grenzflächenforschung – Kernforschungsanlage – Jülich for invaluable help during the construction of the He-scattering apparatus. J. M. Bertosio and G. Antoine have contributed to different stages of the experimental setup, while M. Alnot and M. Robinson have been in charge of the computer work. We would like to express our gratitude to them here. Laboratoire Maurice Letort is associated with University of Nancy I.

¹A. Sanchez, I. Ibanez, R. Miranda, and S. Ferrer, *J. Appl. Phys.* **61**, 1239 (1987).

²J. Henrion and G. E. Rhead, *Surf. Sci.* **29**, 20 (1972).

³A. Sepulveda and G. E. Rhead, *Surf. Sci.* **67**, 436 (1977).

⁴W. C. Marra, P. H. Fuoss, and P. Eisenberger, *Phys. Rev. Lett.* **49**, 1169 (1982).

⁵S. Brennan, P. H. Fuoss, and P. Eisenberger, in *The Structure of Surfaces*, edited by M. A. Van Hove and S. Y. Tong (Springer, Berlin, 1985), p. 421.

⁶K. Kern, R. David, and G. Comsa, *Rev. Sci. Instrum.* **56**, 372 (1985).

⁷B. Poelsema and G. Comsa, in *Scattering of Thermal Energy Atoms*, edited by G. Höhler, Springer Tracts in Modern Physics Vol. 115 (Springer, Berlin, 1989), pp. 12–33.

⁸K. Kern, R. David, R. L. Palmer, and G. Comsa, *Phys. Rev. Lett.* **56**, 620 (1985).

⁹B. Poelsema, L. K. Verheij, and G. Comsa, *Phys. Rev. Lett.* **49**, 1731 (1982).

¹⁰B. Poelsema, L. K. Verheij, and G. Comsa, *Surf. Sci.* **152/153**, 496 (1985).

¹¹R. Manson, private communication to Poelsema and Comsa, as quoted in Ref. 7, p. 22.